DENSITY FUNCTIONAL THEORY INVESTIGATION OF LINEAR CARBON CHAINS

A THESIS SUBMITTED TO
THE GRADUATE SCHOOL OF ENGINEERING AND SCIENCE
OF BILKENT UNIVERSITY
IN PARTIAL FULFILLMENT OF THE REQUIREMENTS FOR
THE DEGREE OF
MASTER OF SCIENCE
IN
PHYSICS

By
Efe Dorukhan Salepci
September 2023

DENSITY FUNCTIONAL THEORY INVESTIGATION OF LINEAR CARBON CHAINS

By Efe Dorukhan Salepci

September 2023

We certify that we have read this thesis and that in our opinion it is fully adequate, in scope and in quality, as a thesis for the degree of Master of Science.

Oğuz Gülseren(Advisor)

Mehmet Cemal Yalabık

Mehmet Emre Taşgın

Approved for the Graduate School of Engineering and Science:

Orhan Arıkan
Director of the Graduate School

ABSTRACT

DENSITY FUNCTIONAL THEORY INVESTIGATION OF LINEAR CARBON CHAINS

Efe Dorukhan Salepci
M.S. in Physics
Advisor: Oğuz Gülseren
September 2023

In this thesis the structural and electronic properties of linear carbon chains are investigated using density functional theory. Polyyne structure of alternating single and triple bonds was shown to be energetically favored structure compared to successive double-double bonded cumulene structure. Band calculations showed that polyyne is a semiconductor whereas cumulene is a metal. Phonon calculations showed that cumulene is unstable. When put in a hexagonal formation these chains are found to form three possibly stable structures, one tightly bound hexagonal tube, and two loosely bound structures one which can be described as a hexagonal assembly of polyyne chains and one which can be considered stacks of hexagonal carbon flakes. Electronic band structure calculations showed that all three structures are semiconductors. Charge density profile showed strong chemical bonds both in vertical and horizontal directions for the first structure, whereas second structure of polyyne chains had no strong bonds between chains and third structure of hexagon flakes showed no strong bond between hexagon flakes. It is also found that as hexagon size shrinks the favored structure of chains changes from polyyne to cumulene and a band structure calculation showed that a semiconductor to metal transition happens.

Keywords: Carbon Linear Chains, Carbyne, Cumulene, Polyyne, Density Functional Theory.

ÖZET

DOĞRUSAL KARBON ZİNCİRLERİNİN YOĞUNLUK FONKSİYONELİ TEORİSİ İLE İNCELENMESİ

Efe Dorukhan Salepci
Fizik, Yüksek Lisans
Tez Danışmanı: Oğuz Gülseren
Eylül 2023

Bu tezde yoğunluk fonksiyoneli teorisi kullanılarak doğrusal karbon zincirlerinin yapısal ve elektronik özellikleri araştırılmaktadır. Sırayla tekli ve üçlü bağlarla bağlı karbon atomlarından oluşan polyyne zincirinin sadece ikili bağlarla bağlı karbon atomlarından oluşan cumulene zincirine göre daha düşük enerjili ve kararlı yapı olduğu gösterilmiştir. Elektron bant hesapları polyyne yapısının yarı iletken, cumulene yapısının ise metal olduğunu göstermiştir. Fonon hesapları cumulene yapısnın kararlı olmadığını göstermiştir. Zincirlerin altıgen düzeninin bir tane sıkıca bağlı altıgen tüp şeklinde ve iki adet hafif bağlı üç olası kararlı yapı oluşturduğu görülmüştür. Hafif bağlı yapılardan ilki karbon zincirlerinin zayıf bir etkileşimle birbirlerine bağlanmasından, ikincisi ise altıgen şeklinde sıkıca birbirine bağlanmış karbon halkalarının zayıf bir bağ ile dikey dizilmesiyle oluşmuştur. Elektron bant hesapları üç yapının da yarı iletken olduğunu göstermiştir. Yük yoğunluğu haritaları ilk yapı için hem yatay hem dikey yönlerde karbonlar arası kuvvetli kimyasal bağlar, ikinci yapı için sadece dikey yönde zincir boyunca kuvvetli bağlar, üçüncü yapı için ise sadece yatay altıgen halkada kuvvetli bağlar göstermiştir. Hexagon boyutu küçüldükçe zincirlerin stabil yapısının polyyne den cumulene e değiştiği, bant hesaplarından da bu sırada yapının yarı iletkenden metale dönüştüğünü göstermiştir.

Anahtar sözcükler: Doğrusal Karbon Zincirleri, Yoğunluk Fonksiyoneli Teorisi.

Acknowledgement

I would like to thank and express my sincere gratitude

to my advisor Prof. Oğuz Gülseren for his support and the valuable guidance he provided through all of my masters journey,

to Dr. Ceren Sibel Sayın for helping me in the process of writing this thesis and patiently teaching me how to navigate the truba system without which half of the calculations in this thesis would not be possible,

to all my family and friends whose love, support and meaning they bring into my life cannot be adequately appreciated, not even remotely, in an acknowledgments page,

and to Bilkent Federal Coffee and its wonderful crew (past and present) who make that vibrant place possible. Federal, where I spent more time than my house and campus (combined!) and where I wrote this thesis, brought much needed joy to the long study sessions that my struggle with physics demanded.

The numerical calculations reported in this thesis were to a considerable extend performed at TUBITAK ULAKBIM, High Performance and Grid Computing Center (TRUBA resources).

Contents

List of Figures

Chapter 1

Introduction

Carbynes (monatomic linear chains of carbon) are elusive allotropes of carbon which are truly one dimensional structures which has garnered much attention due to their exceptional electronic properties like tunable band gap and conductivity that can be changed by inducing stress, strain, torsion or adding different chemical end groups. They also show exceptional mechanical properties such as being the materials having the highest specific tensile strength [2, 3, 4, 5]. These properties make linear carbon chains a very lucrative potential material of choice for applications in a broad range of areas like microelectronics, hydrogen storage and medicine. [6, 7, 8, 9, 10, 11].

There are two varieties of carbyne, one named cumulene with identical double bonds and one named polyyne with alternating single and triple bonds (Figure 1.1). First theorized by Neil W. Ashcroft and N. David Mermin in polyyne form, and later predicted to be stable in 1992 by L. A. Girifalco and M. Hodak, the synthesis of carbynes remained a significant challenge for decades due to their extreme reactivity [12, 13]. However new techniques such as using multi walled carbon nanotubes are enabling synthesis of longer and longer carbon chains [14, 15]. Also, new methods to produce carbon chains by growing them perpendicularly on top of different surfaces are emerging [16, 17]. These new advances are making it crucial to understand the properties of linear carbon chains and interactions

between them in different formations, since understanding these interactions are crucial to predict and suggest the most efficient and promising synthesis methods and stability conditions. Wider analysis is also needed to understand the type of properties these structures will manifest depending on their synthesis routes and final configurations.

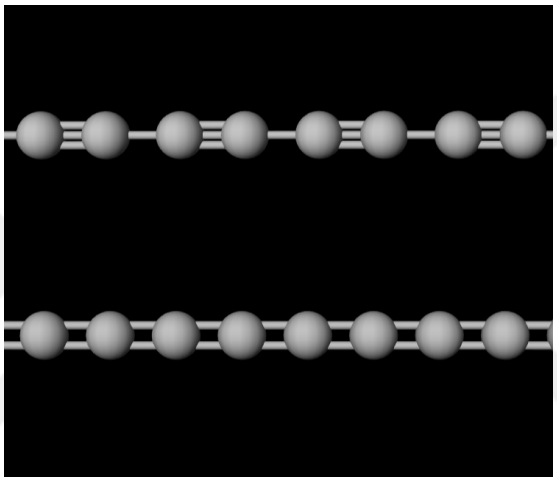

Figure 1.1: Polyyne structure (top) and cumulene (bottom) [1].

In this thesis, after a brief summary of density functional theory, investigation of structural and electronic properties of isolated cumulene and polyyne type linear carbon chains are undertaken, and then a set of relaxation calculations are used to observe behavior of chains under various hexagonal formations. Three different possibly stable structures were spotted and their structural and electronic properties are inspected.

Chapter 2

Theoretical Background

2.1 Many Body Problem

Even though the precise mathematical formulation of an interacting quantum mechanical system is known, when it comes to solving the equations handed us by the theory to reach analytic solutions we bump into a wall known as "the many body problem". This problem manifests itself even in relatively simple theory of Newtonian gravitation where simple solutions cannot be reached for a gravitationally interacting system of more than 2 masses.

The problem is considerably worse if we consider the quantum mechanical description of a macroscopic system of particles on the order of Avogadro's number. Richard Feynman's pioneering work in quantum electrodynamics and the development of quantum field theory highlighted the challenges of understanding the behavior of multiple interacting particles in a quantum context. The quantum many-body problem has profound implications for understanding the behavior of electrons in solids, the behavior of atoms and molecules in chemical reactions, and the properties of exotic states of matter such as Bose-Einstein condensates and strongly correlated electron systems [18, 19, 20, 21].

2.2 Statement of the Problem

The most general description begins with the Schrödinger equation,

$$\hat{H}|\psi\rangle = E|\psi\rangle \tag{2.1}$$

where $|\psi\rangle$ is the wave function and H is the Hamiltonian of the system. For a system of N particles, this function is a complex valued function of 4N variables (3 space coordinates and one spin coordinate for each particle).

In the time independent Schrödinger equation above, $|\psi\rangle$ is an eigenstate of the Hamiltonian H with energy E. Without a magnetic field, and ignoring the smaller effects of spin dependent potential, the Hamiltonian above is,

$$\begin{aligned}\hat{H} = &-\frac{\hbar^2}{2m_e}\sum_i \nabla_i^2 - \sum_{i,I}\frac{Z_I e^2}{4\pi\epsilon_0|\mathbf{r}_i - \mathbf{R}_I|} + \frac{1}{2}\sum_{i\neq j}\frac{e^2}{4\pi\epsilon_0|\mathbf{r}_i - \mathbf{r}_j|} \\ &- \frac{\hbar^2}{2M_I}\sum_I \nabla_I^2 + \frac{1}{2}\sum_{I\neq J}\frac{Z_I Z_J e^2}{4\pi\epsilon_0|\mathbf{R}_I - \mathbf{R}_J|}\end{aligned} \tag{2.2}$$

i, j indices refer to electrons and I, J refer to nuclei, $\mathbf{r}_i, \mathbf{r}_j$ are positions of electrons and $\mathbf{R}_I, \mathbf{R}_J$ are positions of nuclei.

One simplification to the above eigenvalue equation starts with the realization that mass of nuclei is three to four orders of magnitude bigger than that of electron. This means that for most problems of interest we can consider nuclei as static particles, frozen in space. This is called the Born - Oppenheimer approximation [22] and it leads to the following simplified Hamiltonian,

$$\hat{H} = \hat{T} + \hat{V}_{ee} + \hat{V}_{ext} + E_{II} \tag{2.3}$$

Adopting Hartree units where $\hbar = m_e = e = 4\pi\epsilon_0 = 1$, these terms are, the kinetic energy term,

$$\hat{T} = -\frac{1}{2}\sum_i \nabla_i^2 \tag{2.4}$$

the electron-electron interaction term,

$$\hat{V}_{ee} = \frac{1}{2}\sum_{i\neq j} \frac{1}{|\mathbf{r}_i - \mathbf{r}_j|} \tag{2.5}$$

and nuclei-electron interaction term,

$$\hat{V}_{ext} = -\sum_i \sum_I \frac{Z_I}{|\mathbf{r}_i - \mathbf{R}_I|} = \sum_i V_{nuc}(\mathbf{r}_i) \tag{2.6}$$

where $V_{nuc}(\mathbf{r}_i)$ is the potential due to all nuclei in the system.

If we could just solve the eigenvalue problem and find the ground state wave function and energy, we could compute most properties of interest by taking the expectation value of the corresponding operator. But even with Born-Oppenheimer approximation this is an impossibly difficult problem to tackle with a head on fashion. Thus we need to resort to other approaches.

2.3 Basics of DFT

One of the most successful approaches to the many body problem is to reformulate it in terms of electron density,

$$n(\mathbf{r}) = N\sum_\sigma \int\int \psi(\mathbf{r},\sigma,\mathbf{x}_2,\mathbf{x}_3,...,\mathbf{x}_N)\psi^*(\mathbf{r},\sigma,\mathbf{x}_2,\mathbf{x}_3,...,\mathbf{x}_N)d\mathbf{x}_2 d\mathbf{x}_3 ... d\mathbf{x}_N \tag{2.7}$$

where $\mathbf{x}_n = (\mathbf{r}_n, \sigma_n)$ refer to both space and spin coordinates of the n'th particle, so the space coordinate of the first particle $\mathbf{r}$ is not integrated over.

Working with density, which is a function of only 3 variables is vastly easier compared to the many-body wave function of 3N variables.

Hohenberg-Kohn theorems, named after Pierre Hohenberg and Walter Kohn, are the backbones of density functional theory(DFT) [23]:

Theorem I: There is a one to one correspondence between the ground state electron density n and the external potential $\mathbf{V}_{ext}$. Thus, given density n, $\mathbf{V}_{ext}$ and therefore the whole Hamiltonian of the system is determined. This also means that all properties of the system are determined given only the ground state density $n_g(r)$.

Theorem II: A universal functional F_{LL} of density can be defined so that the ground state density is given by the minimum of the following energy functional,

$$E[n] = F_{LL}[n] + \int V_{nuc}(\mathbf{r})n(\mathbf{r})d\mathbf{r} \tag{2.8}$$

2.4 Constrained Search

Constrained search formulation [24, 25] of DFT clarifies the implications of HK theorems.

Energy of the system is given by taking the expectation value of the Hamiltonian,

$$\langle\psi|\hat{H}|\psi\rangle = E \tag{2.9}$$

the ground state is found by minimizing this expression with respect to all anti-symmetric N-body wave functions,

$$\min_{\psi\to N}\langle\psi|\hat{H}|\psi\rangle = E_{GS} \tag{2.10}$$

In constrained search formulation, this minimization is separated into two steps. First, we minimize the energy with respect to all wave functions that give a specific density n,

$$\min_{\psi \to n} \left(\langle \psi | \hat{T} | \psi \rangle + \langle \psi | \hat{V}_{ee} | \psi \rangle + \int V_{nuc}(\mathbf{r}) n(\mathbf{r}) d\mathbf{r} \right) = F_{LL}[n] + \int V_{nuc}(\mathbf{r}) n(\mathbf{r}) d\mathbf{r} \tag{2.11}$$

where F_{LL} is the Levy-Lieb functional,

$$F_{LL}[n] = \min_{\psi \to n} \left(\langle \psi | \hat{T} | \psi \rangle + \langle \psi | \hat{V}_{ee} | \psi \rangle \right) \tag{2.12}$$

Then we minimize this expression with respect to all densities that give the correct number of electrons,

$$E_{GS} = \min_{n \to N} \left(F_{LL}[n] + \int V_{nuc}(\mathbf{r}) n(\mathbf{r}) d\mathbf{r} \right) \tag{2.13}$$

2.5 Kohn-Sham Method

Even though Hohenberg-Kohn theorems provide a link between density and properties of the system, they provide no way to make calculations. Kohn-Sham method provides such a way [26].

The method starts by the assumption that the ground state density of the system can be represented as the density of an auxiliary non-interacting system,

$$n(\mathbf{r}) = \sum_{i=1}^{N} \psi_i(\mathbf{r}) \psi_i^*(\mathbf{r}) \tag{2.14}$$

where ψ_i are the single particle states occupied by the non-interacting electrons.

Single particle states will be the eigenstates of the auxiliary Hamiltonian,

$$\hat{H}_{aux} = \hat{T}_s + \hat{V}_{eff} \tag{2.15}$$

so that,

$$\hat{H}_{aux} \psi_i(\mathbf{r}) = \epsilon_i \psi_i(\mathbf{r}) \tag{2.16}$$

$\hat{T}_s$ is the usual kinetic energy operator $-\frac{1}{2}\nabla^2$, what $\hat{V}_{eff}$ means will be shown soon.

Our aim is to find the density n that minimizes the energy functional (8). We can re-write this functional in the following manner,

$$E[n] = T_s[n] + E_H[n] + E_{xc}[n] + \int V_{nuc}(\mathbf{r})n(\mathbf{r})d\mathbf{r} \tag{2.17}$$

where $T_s[n]$ is the independent particle kinetic energy,

$$T_s[n] = -\frac{1}{2}\sum_i \langle\psi_i|\nabla^2|\psi_i\rangle \tag{2.18}$$

even though it is expressed in terms of wave functions, it can be shown that it is a unique functional of the density.

E_H is the Hartree energy, a classical formulation of electron-electron Coulomb repulsion energy associated with the density,

$$E_H[n] = \int\int \frac{n(\mathbf{r})n(\mathbf{r})}{|\mathbf{r}-\mathbf{r}'|}d\mathbf{r}d\mathbf{r}' \tag{2.19}$$

and $E_{xc}[n]$ is the exchange-correlation functional,

$$E_{xc} = F_{LL}[n] - T_s[n] - E_H[n] \tag{2.20}$$

The reason we reformulate the energy functional this way is because the unknown functional $F_{LL}[n]$ is much bigger compared to the unknown functional E_{xc} since Hartree energy $E_H[n]$ is the biggest contributor to the electron-electron interaction energy $\langle\psi|V_{ee}|\psi\rangle$. Therefore the magnitude of the functional we are trying to approximate is going to be smaller and any error in the approximation is expected to be on a smaller magnitude.

Since we are minimizing energy functional with respect to density, we need the functional derivative with respect to eigenstates to vanish,

$$\frac{\delta E[n]}{\delta \psi_i^*(\mathbf{r})} = \frac{\delta T_s}{\delta \psi_i^*(\mathbf{r})} + \left[\frac{\delta E_{ext}}{\delta n(\mathbf{r})} + \frac{\delta E_H}{\delta n(\mathbf{r})} + \frac{\delta E_{xc}}{\delta n(\mathbf{r})}\right] \frac{\delta n(\mathbf{r})}{\delta \psi_i^*(\mathbf{r})} = 0 \tag{2.21}$$

with the orthonormalization constraint $\langle \psi_i | \psi_j \rangle = \delta_{ij}$ this variational equation leads to the Kohn-Sham Schrödinger like equations,

$$(H_{aux} - \epsilon_i)\, \psi_i(\mathbf{r}) = 0 \tag{2.22}$$

with

$$H_{aux} = -\frac{1}{2}\nabla^2 + V_{nuc}(\mathbf{r}) + V_H(\mathbf{r}) + V_{xc}(\mathbf{r}) \tag{2.23}$$

where

$$V_H(\mathbf{r}) = \frac{\delta E_H}{\delta n(\mathbf{r})} \tag{2.24}$$

and

$$V_{xc}(\mathbf{r}) = \frac{\delta E_{xc}}{\delta n(\mathbf{r})} \tag{2.25}$$

so that V_{eff} in equation (15) becomes ,

$$V_{eff} = V_{nuc}(\mathbf{r}) + V_H(\mathbf{r}) + V_{xc}(\mathbf{r}) \tag{2.26}$$

V_H and V_{xc} are density dependent potentials, which means that Kohn-Sham equations (22) have to be solved self consistently. The scheme is as follows: an input density determines the auxiliary Hamiltonian and the solution of Kohn-Sham equations with this new Hamiltonian leads to a new output density. This scheme is repeated until input density and output density converge to each other.

$$... \rightarrow n_i \rightarrow H_{aux_i} \rightarrow n_{i+1} \rightarrow H_{aux_{i+1}} \rightarrow ... \tag{2.27}$$

Determining n_{i+1} is not as straightforward as taking the density given by the solution to H_{aux_i} as n_{i+1} . If we denominate the density given by the solution to H_{aux_i} as n_{out_i} there are different mixing schemes to cook up n_{i+1} using n_i and n_{out_i}. One common method is linear mixing, in which n_{i+1} is given as a linear combination of n_{out_i} and n_i,

$$n_{i+1} = (1 - b)n_i + bn_{out_i} \tag{2.28}$$

where b is usually called the mixing parameter or mixing beta.

2.6 Exchange-Correlation Functional

Exchange-correlation function, whose exact form is unknown and which must be very complicated, can be approximated on different levels. The starting point is called local density approximation (LDA) where the approximating functional uses only the value of the density at each point [27], which is of the form,

$$E_{xc}[n] = \int \epsilon_{xc}\left(n(\mathbf{r})\right) d\mathbf{r} \tag{2.29}$$

where ϵ_{xc} is some function whose form is determined from the homogeneous electron gas system.

The next level, which is the one that is used in the dft model in this thesis, is named generalized gradient approximation (GGA) in which the approximation to the exchange-correlation functional also uses the gradient of the density [28],

$$E_{xc}[n] = \int \epsilon_{xc}\left(n(\mathbf{r}), \nabla n(\mathbf{r})\right) d\mathbf{r} \tag{2.30}$$

2.7 Plane-wave Basis

To solve Kohn-Sham equations we can diagonalize the auxiliary Hamiltonian with respect to a basis set which completely spans the space of possible wave functions for the specified system. One possible basis set is the set of plane waves [29] of the form

$$\psi_{\mathbf{G}}(\mathbf{r}) = e^{-i\mathbf{G}.\mathbf{r}} \tag{2.31}$$

where $\mathbf{G}$ is an element of the reciprocal lattice of the lattice in which the $\hat{V}_{ext}$ is periodic. So that

$$\mathbf{G} = n_1\mathbf{b}_1 + n_2\mathbf{b}_2 + n_3\mathbf{b}_3 \qquad n_1, n_2, n_3 \in \mathbb{Z} \tag{2.32}$$

where b_1, b_2, b_3 are the basis vectors of the reciprocal lattice, defined as

$$\mathbf{b}_1 = \frac{2\pi}{V}\mathbf{a}_2 \times \mathbf{a}_3 \tag{2.33}$$

$$\mathbf{b}_2 = \frac{2\pi}{V}\mathbf{a}_3 \times \mathbf{a}_1 \tag{2.34}$$

$$\mathbf{b}_3 = \frac{2\pi}{V}\mathbf{a}_1 \times \mathbf{a}_2 \tag{2.35}$$

Where $\mathbf{a}_1, \mathbf{a}_2, \mathbf{a}_3$ are basis vectors of the real lattice and V is the volume of the unit cell of real lattice.

Of course, in practice an infinite set of plane waves cannot be used and we have to limit the size of basis set somehow so that calculations finish in a reasonable time. Since the kinetic energy of a plane wave for electrons is given by

$$E = \frac{\hbar^2|\mathbf{G}|^2}{2m_e} \tag{2.36}$$

an energy cutoff value is usually employed to limit the basis set.

2.8 Pseudo-Potential Method

Generally speaking, it is the valance electrons of the constituent atoms that determine the properties of molecules and materials. Inner shell electrons are usually undisturbed by the environment, which means that we can treat the nucleus and inner shell electrons as a whole by changing the nuclear potentials by a prefabricated "pseudo potential" [30].

This approximation helps in two ways. First, we have less electrons to deal with since inner shell electron effects are incorporated into the pseudo potential. Secondly, pseudo potentials get rid of the difficulty associated with the singularities in nuclear potentials. The highly oscillating nature of electronic wave functions near nucleus requires an unnecessarily big set of basis functions to approximate, thus, if we get rid of the necessity to approximate inner shell electron wave functions we can do away with a much smaller basis set size.

2.9 Supercells

Use of plane wave basis in solving Kohn-Sham equations assumes that the underlying structure is periodic in a three dimensional lattice. To meet this assumption, isolated molecules or infinite structures of dimensions less than three requires use of cells that are much longer in certain directions compared to the molecule or the material that is being studied by DFT software. Assuming there can't be much interaction over very long distances (long compared to the system that is being studied), this approach allows the use of methods based on periodicity of the underlying system while preventing the interaction between the periodic copies of the structure. If a free molecule is being studied, the corresponding supercell has to be very long in all three directions, for 2 dimensional film like materials (e.g. graphene) the supercell has to be very long in direction perpendicular to the surface whereas in our case of studying 1 dimensional chain like structures, the supercell has to be large in directions that are perpendicular to the axis of

the 1-D structure.

2.10 Brillouin zone sampling

Many properties of interest depend on integrals over the Brillouin zone. Computationally all integrals (unless the underlying function has an easy analytical integral) must be approximated by Riemann sums which means that to take integrals over Brillouin zone, wee have to sample the Brillouin zone by a finite set of points. One method is to sample the Brillouin zone by an $n_1 \times n_2 \times n_3$ grid which would make $n_1 n_2 n_3$ number of points. Most integrands won't change much over small stretches of Brillouin zone so we can choose grid dimensions proportional to the dimensions of the Brillouin zone. Which means over directions where the Brillouin zone is big, we have to sample it more. The size of Brillouin zone in a certain direction is inversely proporsional to the size of the unit cell in that direction. This means that we need to have more sample points over the directions where the unit cell is small and less sample points over the directions where it is big. If we consider supercells, where the unit cell is very big in at least one direction by definition, we can get away by sampling the Brillouin zone in that direction by a single partition. So if we use a supercell where the cell is very big in x and y direction, we can use a $1 \times 1 \times n_3$ grid.

Chapter 3

Properties of Linear Carbon Chains

In this thesis the structural and electronic properties of the Carbyne first in isolated forms and then in various hexagonal formations are investigated using first-principles plane-wave calculations carried out within the density-functional theory, employing projector augmented wave (PAW) potentials [31], the one in [32] specifically, and a generalized gradient approximation for exchange correlation functional using Perdew-Burke-Ernzerhof (PBE) functional [28], implemented by Quantum ESPRESSO software [33]. All calculations are performed for 0 K.

3.1 The Infinite Chain

Marzari-Vanderbilt-Devita-Payne cold smearing [34] of 0.005 Ry was used for calculations and the self-consistent energy error threshold was set to 10e-8 Ry. Convergence tests showed that a kinetic energy cut off of 50 Ry and k mesh of 1x1x30 provided sufficient accuracy. To model the infinite chain a supercell of rectangular pyramid shape with a 10 Å x 10 Å square base with variable height

in z direction (which will be referred as cell length) is used where the chain axis lies along the z direction. Each cell contains two carbon atoms where exact setup is shown in Figure 3.1.

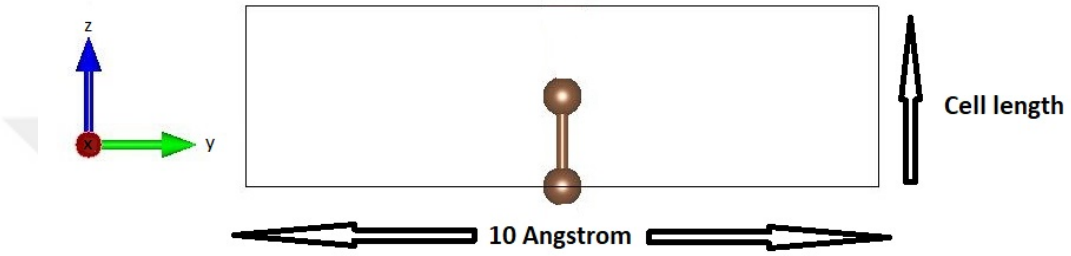

Figure 3.1: Supercell structure.

For calculations of cumulene structure second carbon atom is placed in exactly the middle of the cell length (0.0, 0.0, 0.5) above the first one which is placed on the origin (0.0, 0.0, 0.0). For calculations of polyyne structure z coordinate of the second atom was set as a free variable (0.0, 0.0, b) to be determined by the ionic relaxation at the minimum energy configuration. Atomic force threshold for convergence was set as 1e-5 Ry/au. Preliminary crude calculations hinted at energy minimums around cell length of 2.5 Å and a denser set of calculations were made around this region for both structures which revealed the energy curve in Figure 3.2. The minimum energy -18.3716 Ry per carbon atom for cumulene structure is at 2.564 Å cell length which means bond length is 1.282 Å between carbon atoms. The minimum energy -18.3719 Ry per carbon atom for polyyne is found to be at 2.566 Å cell length and the z coordinate of second atom was found as b = 0.4905 which translates to a shorter "triple" bond of 1.259 Å and a longer "single" bond of 1.307 Å. These results show that polyyne structure is energetically favored by 3e-4 Ry per carbon atom, in accordance with previous studies [35, 36]. Polyyne is also longer "per carbon" by about 0.07% compared to cumulene.

Phonon band structure, electronic band structure, density of states and charge density were calculated and plotted for the minimum energy configurations of

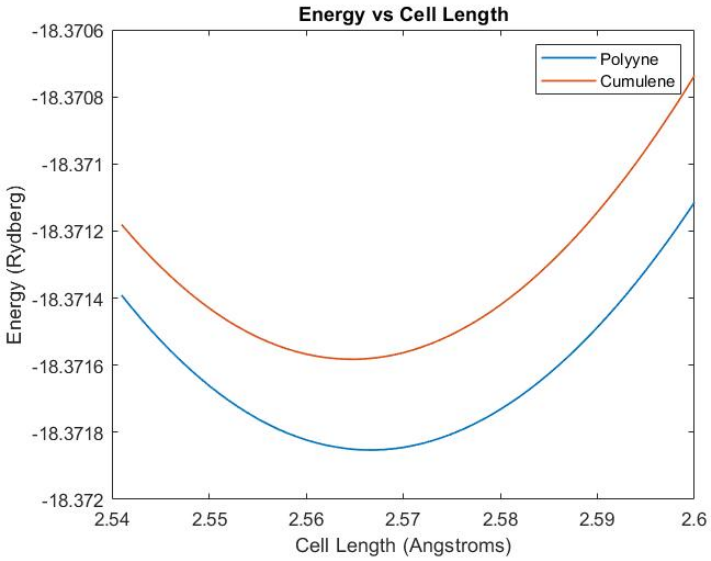

Figure 3.2: Dependence of energy per carbon atom on cell length for polyyne (blue line) and cumulene (orange line).

cumulene and polyyne as presented in Figures 3.3 to 3.6.

Figure 3.3 shows the Phonon band structure of both structures, where presence of imaginary frequencies (represented as negative in figure) in cumulene phonon bands hints at the instability of cumulene structure, whereas for polyyne small negative frequencies only manifest as numerical artifacts. Which is an expected result since ionic relaxation does find the position of the atom up until the force convergence threshold. Any small instability can also be accounted for by factors such as external field, temperature or strain. These results are in agreement with previous calculations [35].

Comparison of charge density maps of cumulene and polyyne is shown in Figure 3.4. Charge density graphs are plotted as the difference between the electron density of the chain structure and the superposed electron density of free carbon atoms. The asymmetries in the figure point at the alternating nature of the bonds in polyyne.

Band structure calculations and the corresponding density of states (DOS) plots are presented in Figure 3.5 and Figure 3.6. As seen in Figure 3.5, a band

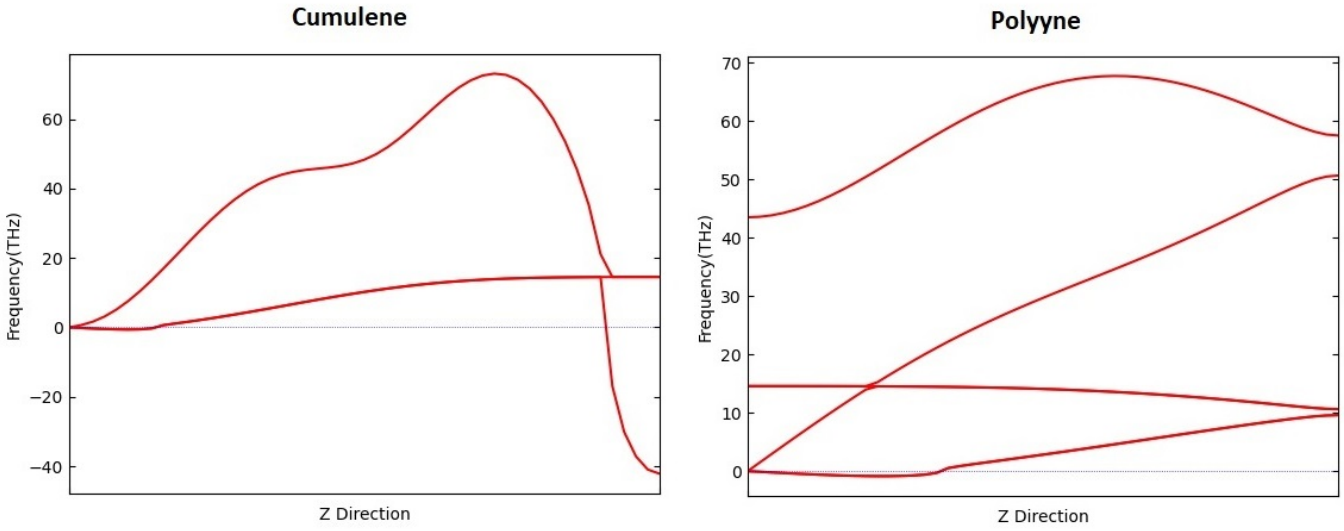

Figure 3.3: Phonon band structure for cumulene (left) and polyyne (right).

gap at fermi level for cumulene does not open which points at its metallic nature. Whereas there exists a small band gap for polyyne structure which we calculated to be about 0.4 eV at Fermi level which means polyyne is a semiconductor in accordance with previous studies [36]. The metallic nature of cumulene and semiconducting nature of polyyne are also reflected in DOS plots where an absence of any states above fermi level (-4.5 eV) for about 0.4 eV in polyyne can be seen.

3.2 Hexagonal Structures of Infinite Chains

3.2.1 Structural properties

Next, the properties of infinite chains arranged in a hexagonal form was investigated. First the cumulenic hexagonal structure as shown in Figure 3.13a was investigated using a supercell of rectangular pyramid shape with a 25 Å x 25 Å square base with variable height in z direction (which will be referred as cell length and in this case also corresponds to the bond length of the chain) where the hexagonal structure axis lies along the z direction. Each cell contains 6 carbon

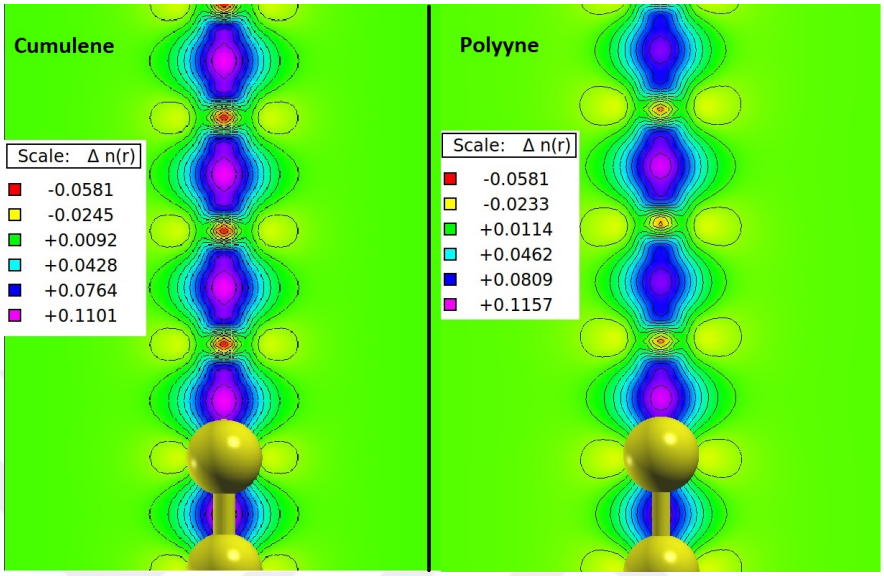

Figure 3.4: Charge density plot for Cumulene(left) and Polyyne(rigth).

atoms where exact setup is shown in Figure 3.7a.

A 3D energy surface was constructed for hexagonal cumulene by varying the cell length between 1 Å and 2.3 Å and the hexagon side length between 1 Å and 3 Å as shown in Figure 3.8. The minimum of the surface which corresponds to a possibly stable structure, is at around 1.63 Å cell length and a hexagon side length of 1.57 Å. Computations with larger hexagon side length turned out to be difficult because of convergence problems which were overcome by setting smearing width to 0.01 Ry, mixing parameter to 0.5 and number of bands to 20.

A separate potential energy surface was not constructed for polyyne hexagonal structure but to see whether it is the polyyne or cumulene form favored in hexagonal structure, a series of variable cell relaxation calculations (vc-relax) were conducted. The supercell used for this set of calculations were created by placing another hexagon carbon formation on top of the first one (Figure 3.8b) where the z coordinates of atoms were released for ionic relaxation. The cell length (this time cell length corresponds to the distance between next nearest neighbor carbon atoms in the chain) was also a free parameter of the vc-relax calculation where the convergence threshold for pressure was set to 0.02 kPa. Convergence threshold for atomic forces was set to 1e-3 Ry/au. Since new supercell was longer

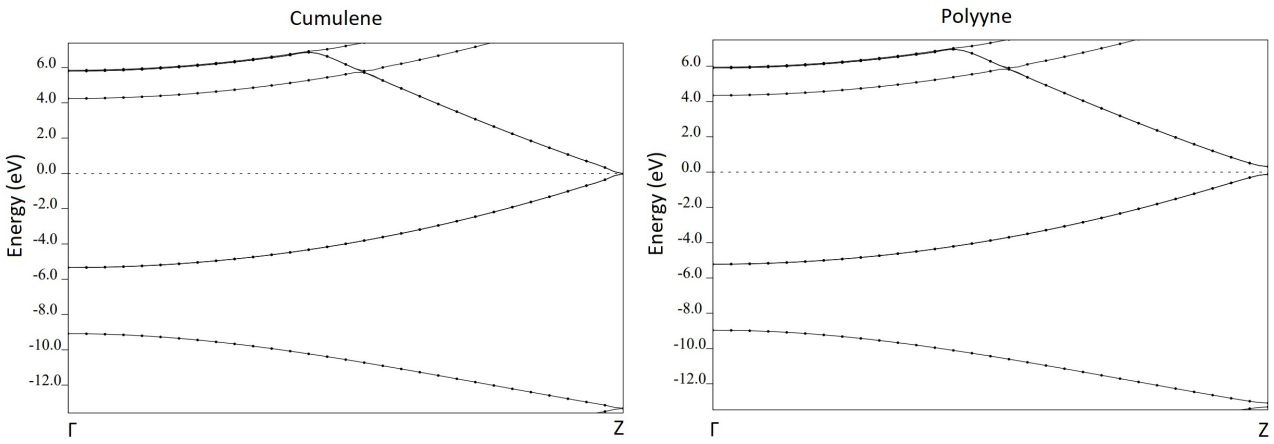

Figure 3.5: Electronic band structure for cumulene(left) and polyyne(right), dotted lines indicate fermi level.

in z direction, a reduced k-point mesh of 1x1x20 was used to reduce computation time.

The following properties of the structure was found as hexagon side length varied from 1.45 Å to 6 Å energy (per carbon atom) (Figure 3.9), cell length (Figure 3.10) and the distance between two hexagons of the cell (expressed as the ratio to cell length, i.e. 0.5 means cumulene with equal bond lengths) which will be referred as Z parameter (Figure 3.11).

These results show that as polyyne chains come closer, there is an energy minimum of about 9.47e-5 Ry at 4.2 Å which hints at hexagonal arrangement of polyyne chains weakly bound by Van der Waals forces. Z parameter plot show that for chains closer than 3.8 Å polyyne structure is no longer favored and cumulene chains are energetically favored. Cell length of the chain stays about the same until chains come closer than 1.85 Å at which point structure changes abruptly to a structure that can be described as a hexagonal tube made of carbon atoms. The minimum energy configuration in 1.45 - 1.8 Å region is at 1.57 Å hexagon side length and 3.24 Å cell length which is the same configuration that was found as the energy minimum of the energy surface constructed before.

Next, to test the stability of the structures of these two energy minimums a full vc-relaxation calculation was done for each structure, leaving cell length

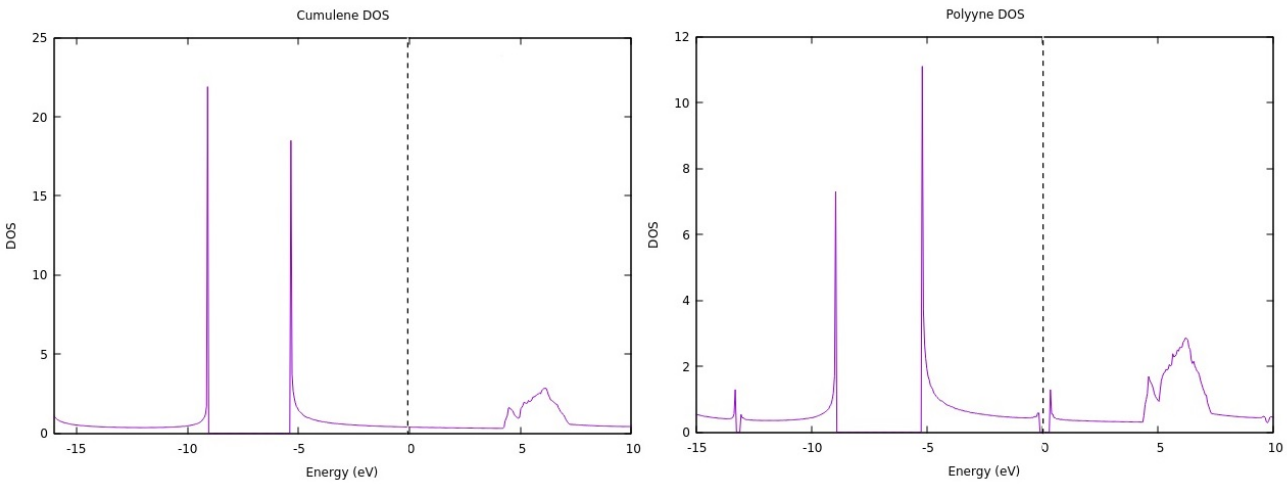

Figure 3.6: Density of states for cumulene(left) and polyyne(right). Dotted line indicates fermi level.

and all coordinates of all carbon atoms as free variables and observing whether energy minimization changed any of these variables. Since both calculations left all variables unchanged it can be concluded that these two structures are indeed stable (at least on the order of energy fluctuations in vc-relax algorithm).

Another series of calculations of hexagonal cumulene structure were done, where the hexagonal side length was set to 1.57 Å while the cell length (also the bond length of chains since this is a cumulene structure with only one hexagon inside the cell) changed from 1 Å to 3 Å which revealed a third possible structure at cell length of 2.8 Å (Figure 3.12). However a vc-relax calculation where z coordinates of carbon atoms and the cell length were left as free variables showed that this structure relaxes to one with a hexagon side length of 1.31 and a cell length of 4.10 Å. This structure can be interpreted as hexagonal carbon flakes held by weak Van der Waals forces. To the knowledge of the author, there are no previous studies that computationally studied the properties of these hexagonal structures.

An illustration of these three structures can be seen in Figure 3.13.

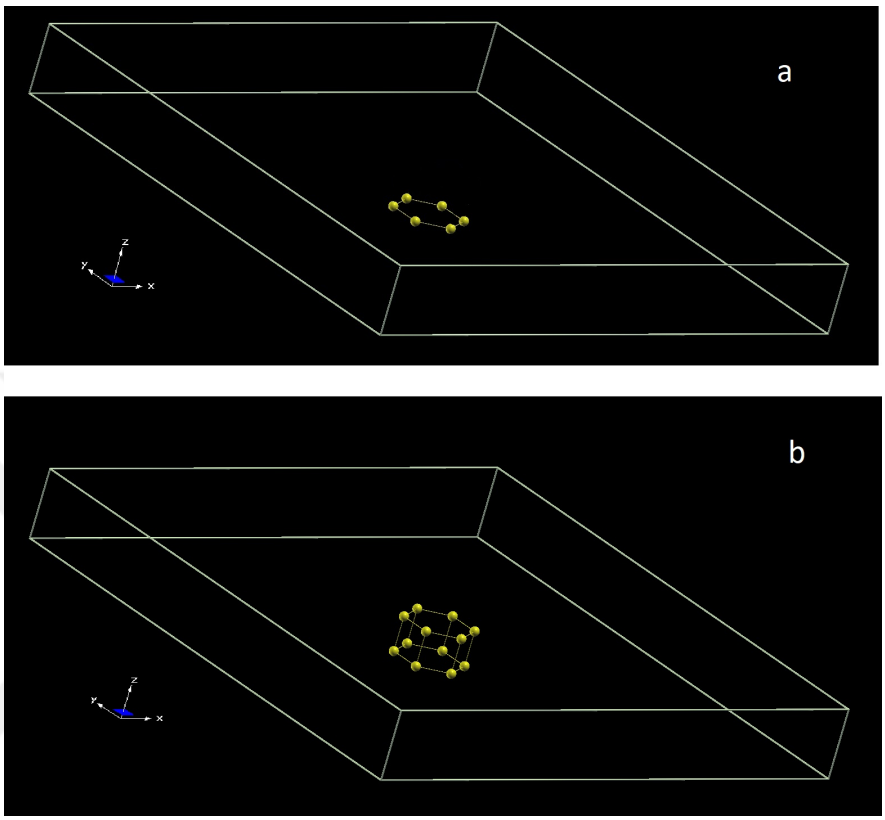

Figure 3.7: Cells used for hexagonal structure calculations for cumulene (top) and for calculations involving ionic relaxation (bottom)

3.2.2 Electronic Properties

Finally band structure and charge density were calculated for these three structures. The results can be seen for the tightly bound hexagonal tube in Figure 3.14 and Figure 3.15, where presence of high electron density regions between carbon atoms in both vertical and horizontal directions show that this structure is indeed bonded by strong chemical bonds. Band structure also shows a band gap of about 0.3 eV so that this structure is a semiconductor.

For weakly bound polyyne chain, Figure 3.17 show that charge density are basically the same with the free polyyne chain which also shows that these chains are indeed only weekly interacting since spaces between the chains show no difference in charge density from the superposition of free carbon atoms. The band structure in Figure 3.16 also show almost the same pattern with the individual

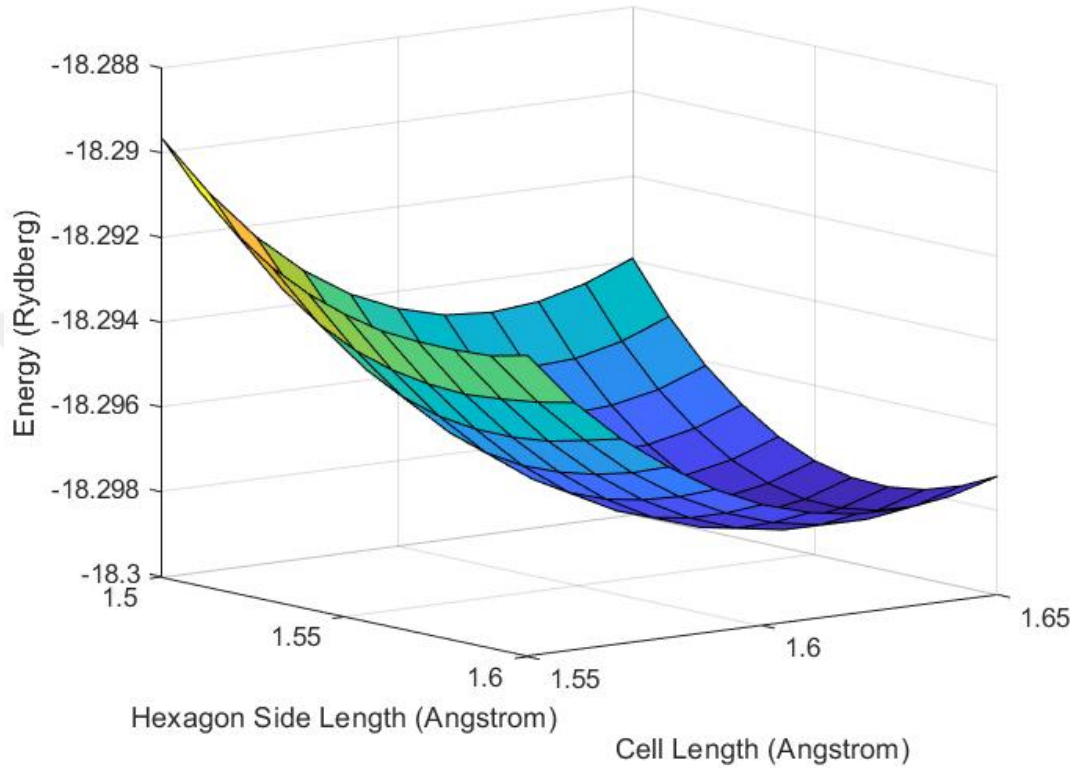

Figure 3.8: Energy surface for cumulenic hexagon.

polyyne chain which is expected due to very limited interaction.

For hexagon carbon flakes in Figure 3.19 charge density plot shows strong bonding inside hexagon flakes but very little interaction between individual flakes which is also reflected in band structure profile of Figure 3.18 which show mostly flat bands which is expected since on Z direction individual flakes are barely interacting which makes it hard for vibrations to propagate in that direction.

Seeing the transition from polyyne to cumulene as the hexagon side length shrinks to below 3.8 Å one final calculation of band structure at 3.0 Å hexagon side showed that there is no band gap for this structure (Figure 3.20). This means that at around 3.8 Å structure changes from a semiconductor to metal, so applying pressure on horizontal directions to chain axis may induce a semiconductor to metal transition.

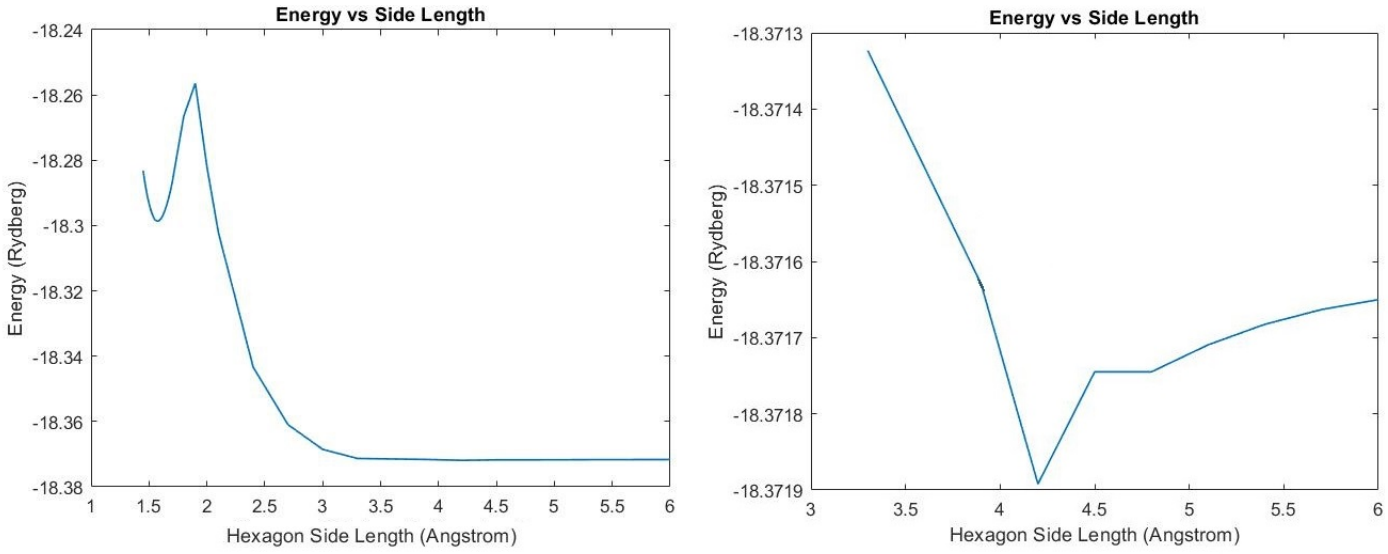

Figure 3.9: Energy vs side length, second plot on the right zooms into the 3 Å - 6 Å region to reveal the second minimum.

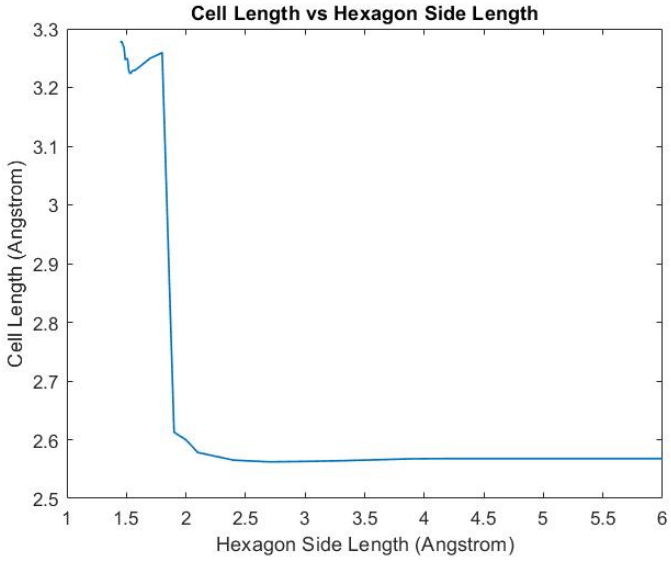

Figure 3.10: Cell length of the relaxed structure vs side length of hexagon.

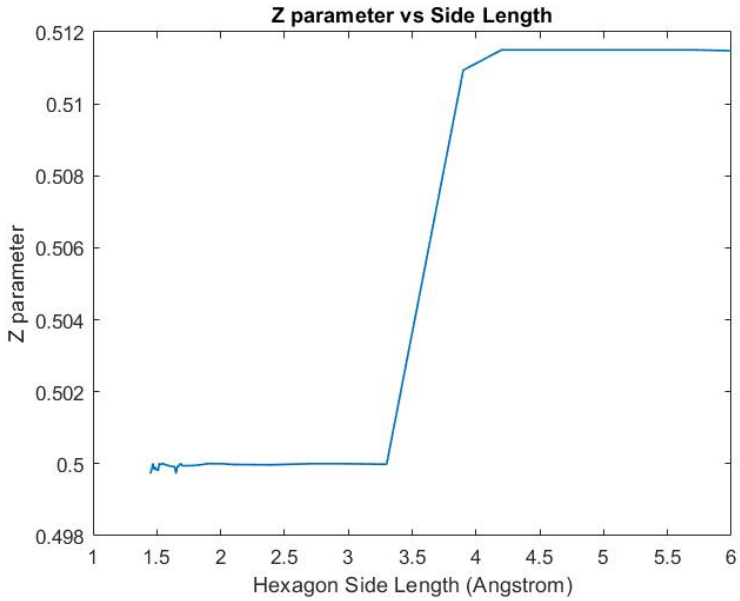

Figure 3.11: Z parameter vs hexagon side length.

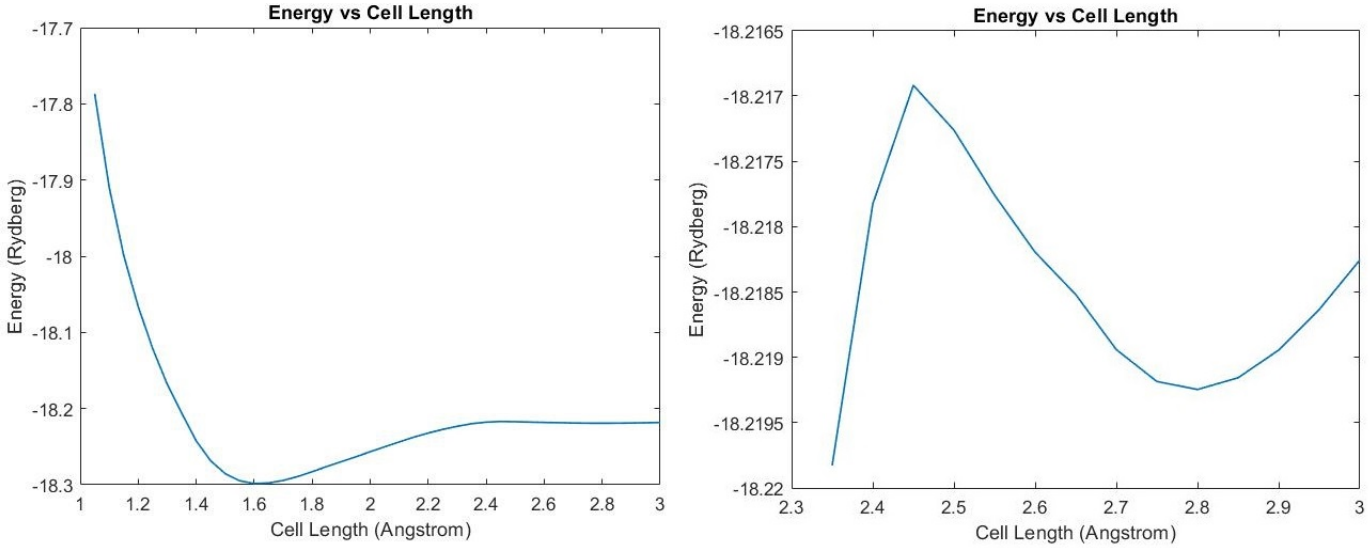

Figure 3.12: Energy vs cell length where hexagon side is kept fixed at 1.57 Å second plot on the right closes up to 2.3 Å - 3 Å region to reveal the energy minimum.

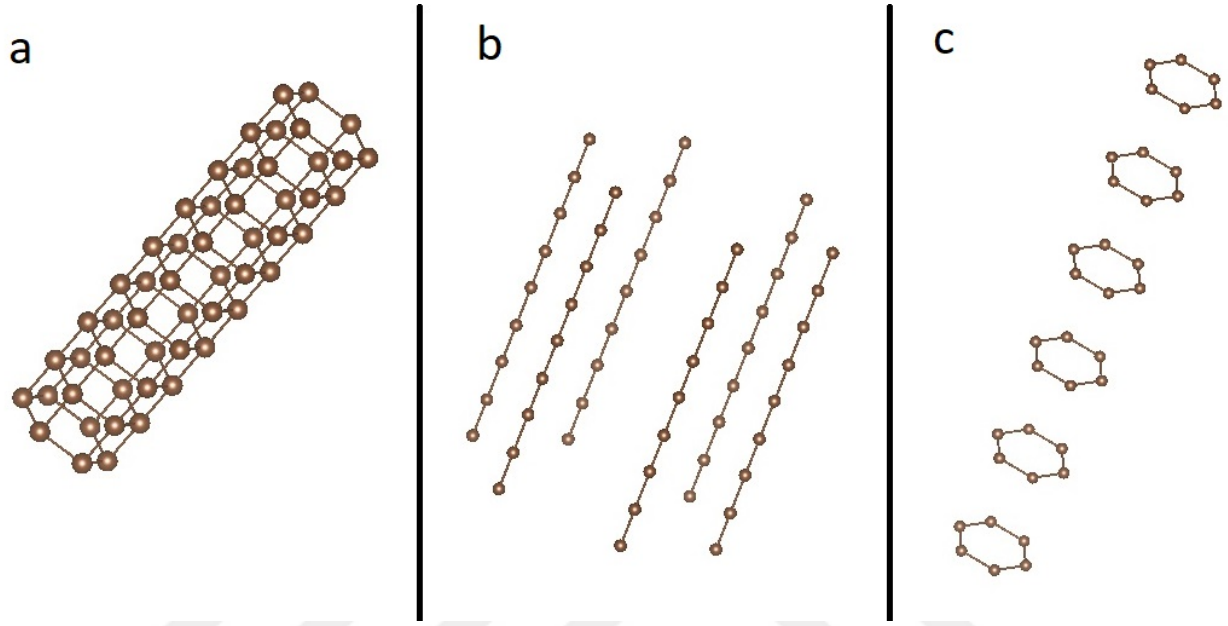

Figure 3.13: Illustration of three structures corresponding to local energy minima, a) The tightly bound hexagonal tube. b) Loosely bound polyyne chains in hexagon formation. c) Loosely bound hexagon flakes.

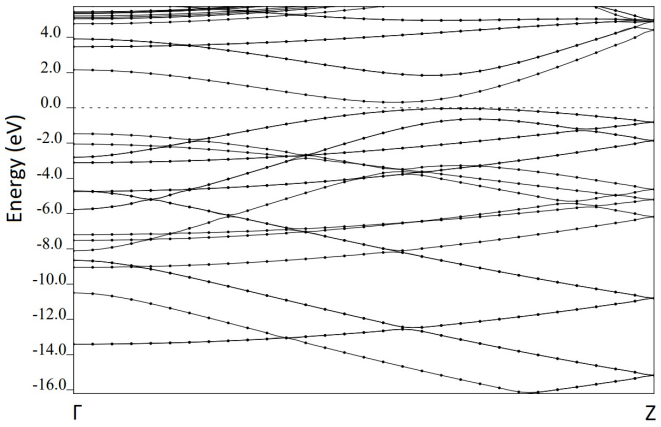

Figure 3.14: Band structure for the hexagonal tube, dotted line indicates the fermi level.

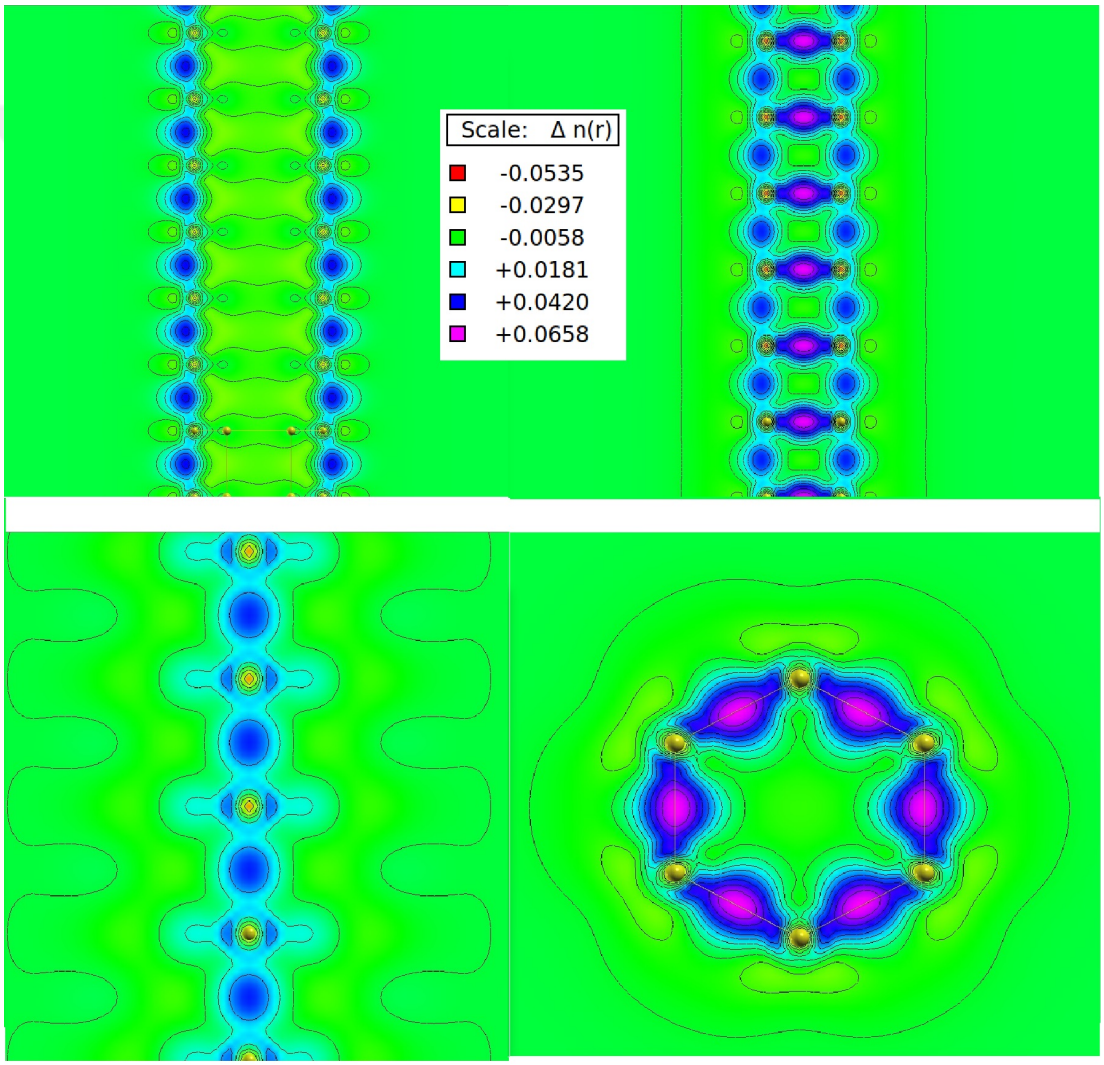

Figure 3.15: Hexagonal tube charge density plotted for different cross sections.

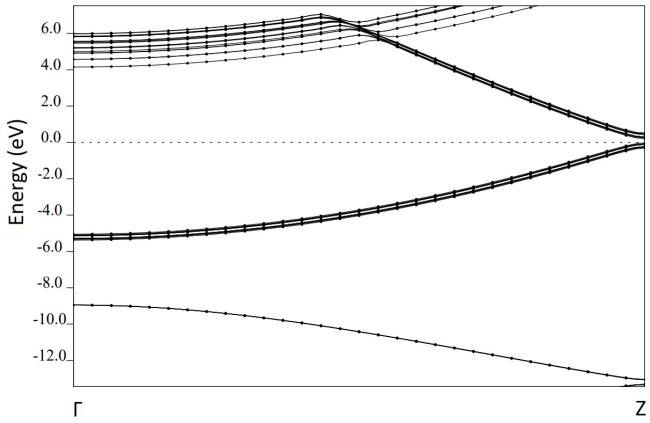

Figure 3.16: Band structure for the weakly bound hexagonal polyyne chains, dotted line indicates the fermi level.

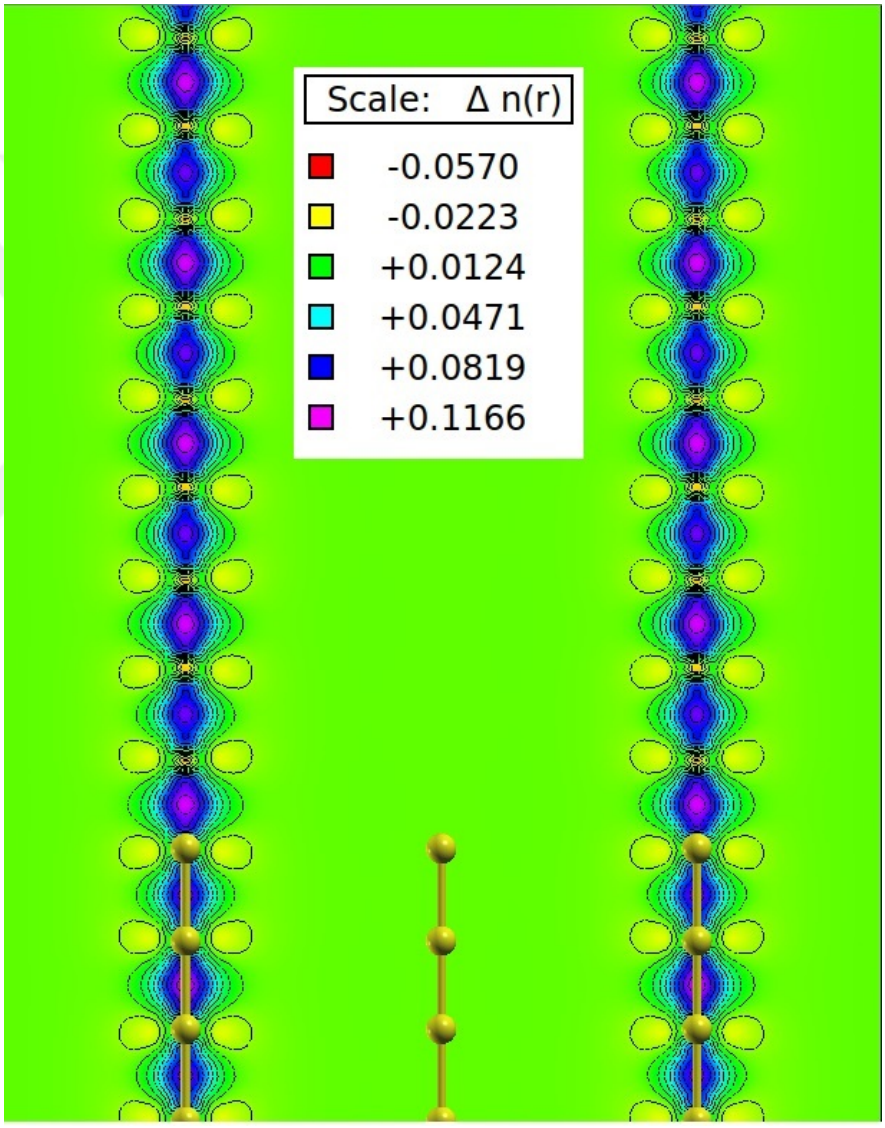

Figure 3.17: Charge density plot for loosely bound hexagonal formation of polyyne chains.

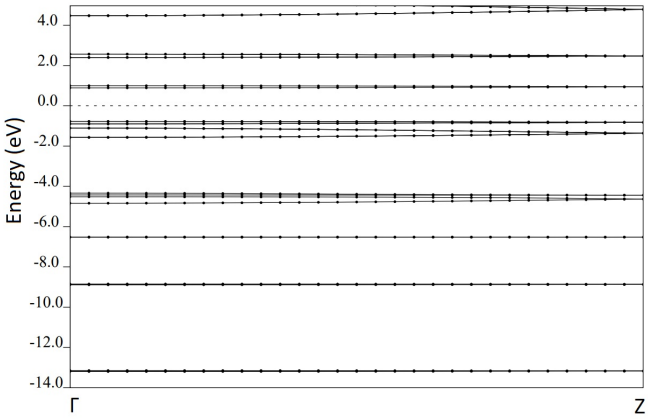

Figure 3.18: Band structure for the hexagon carbon flake structure, dotted line indicates the fermi level.

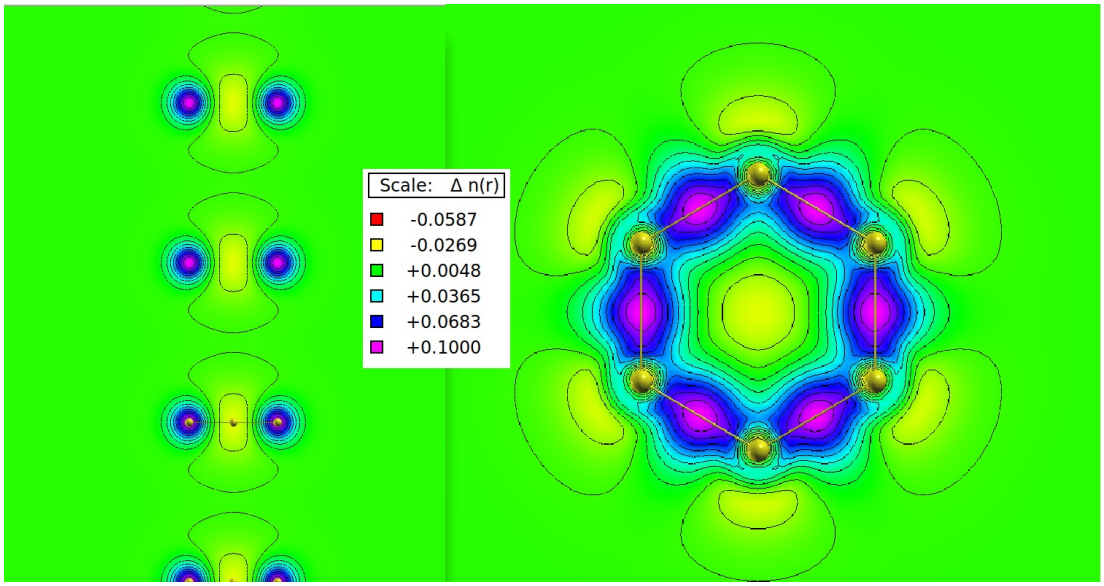

Figure 3.19: Hexagon carbon flake charge density plotted for different cross sections.

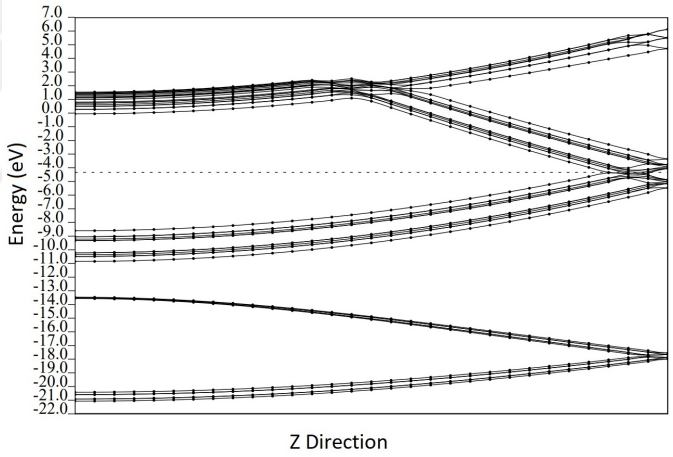

Figure 3.20: Band structure of hexagonal formation of cumulene chains at 3.0 Å hexagon side length.

Chapter 4

Conclusion

Supercell calculations using ionic relaxation of free infinite chain of carbons in forms of polyyne and cumulene showed that polyyne form was energetically favorable to the cumulene form with an altering bond length of 1.307 Å and 1.259 Å at minimum energy configuration compared to 1.282 Å of cumulene which also means that chain is slightly longer per carbon atom in polyyne form compared to the cumulene form. Energy difference between the two is 3e-4 Ry per carbon atom. Phonon band calculations also showed imaginary frequencies which confirms the instability of the infinite cumulene chain. Electronic band calculations showed no band gap at fermi level of cumulene form whereas there was a band gap of about 0.4 eV in polyyne case which can be interpreted as cumulene being a metal and polyyne a semiconductor.

Energy surface construction for hexagonal formation of cumulene chains showed a minimum at 1.57 Å hexagon side length and 1.63 Å chain bond length. This structure, which can be considered as a hexagonal tube of carbon atoms, was shown to be stable by a variable cell relaxation calculation in which energy minimization with respect to all coordinates of carbon atoms and cell length resulted in exactly same coordinates for atoms and an only marginally modified cell length of 1.614 Å compared to the 1.63 Å of the starting configuration.

Further exploration of this energy minimum by keeping hexagon side length fixed at 1.57 Å while increasing the cell length showed a shallow energy minimum at a cell length of 2.8 Å however a variable-cell ionic relaxation calculation starting from this configuration showed that this structure was not stable and the resulting stable configuration resulted in a hexagon side length of 1.31 Å and cell length of 4.1 Å which can be described as stacked hexagonal carbon flakes.

Another set of variable-cell relaxations exploring the energy of the structure as the hexagon side length changed from 1.45 Å to 6 Å revealed two energy minima first one at 1.57 Å which corresponds to the tubular structure discussed above and a second one at 4.2 Å with a cell length of 2.68 Å which corresponds to the cell length of polyyne chain. The vertical distance between carbon atoms in the second energy minimum also revealed alternating bond lengths of 1.31 Å and 1.26 Å so that this structure can be considered as a hexagonal formation of loosely bound polyyne chains.

The same set of variable-cell relaxation calculations also revealed that polyyne formation of carbon chains with alternating bond length were favorable as in the free chain case up until the chains got closer than 3.8 Å after which the cumulene structure was the energetically favorable form. A band structure calculation at 3 Å hexagon side length showed that hexagonal formation of cumulene chains is metallic and a possible semiconductor to metal transition happens as the hexagon shrinks below 3.8 Å.

Bibliography

[1] "Figure created using molview." https://molview.org. Accessed on 11/9/2023.

[2] F. Banhart, "Chains of carbon atoms: A vision or a new nanomaterial?," *Beilstein Journal of Nanotechnology*, vol. 6, pp. 559–569, 2015.

[3] L. Ravagnan, N. Manini, E. Cinquanta, G. Onida, D. Sangalli, C. Motta, M. Devetta, A. Bordoni, P. Piseri, and P. Milani, "Effect of axial torsion on *sp* carbon atomic wires," *Phys. Rev. Lett.*, vol. 102, p. 245502, Jun 2009.

[4] E. Cinquanta, L. Ravagnan, I. E. Castelli, F. Cataldo, N. Manini, G. Onida, and P. Milani, "Vibrational characterization of dinaphthylpolyynes: A model system for the study of end-capped isp/i carbon chains," *The Journal of Chemical Physics*, vol. 135, nov 2011.

[5] E. Durgun, R. T. Senger, H. Mehrez, S. Dag, and S. Ciraci, "Nanospintronic properties of carbon-cobalt atomic chains," *Europhysics Letters*, vol. 73, p. 642, jan 2006.

[6] Y. Wang, X.-J. Ning, Z.-Z. Lin, P. Li, and J. Zhuang, "Preparation of long monatomic carbon chains: Molecular dynamics studies," *Phys. Rev. B*, vol. 76, p. 165423, Oct 2007.

[7] E. Erdogan, I. Popov, C. G. Rocha, G. Cuniberti, S. Roche, and G. Seifert, "Engineering carbon chains from mechanically stretched graphene-based materials," *Phys. Rev. B*, vol. 83, p. 041401, Jan 2011.

[8] A. G. Rinzler, J. H. Hafner, P. Nikolaev, P. Nordlander, D. T. Colbert, R. E. Smalley, L. Lou, S. G. Kim, and D. Tománek, "Unraveling nanotubes: Field emission from an atomic wire," *Science*, vol. 269, no. 5230, pp. 1550–1553, 1995.

[9] N. D. Lang and P. Avouris, "Oscillatory conductance of carbon-atom wires," *Phys. Rev. Lett.*, vol. 81, pp. 3515–3518, Oct 1998.

[10] A. Yazdani, D. M. Eigler, and N. D. Lang, "Off-resonance conduction through atomic wires," *Science*, vol. 272, no. 5270, pp. 1921–1924, 1996.

[11] P. B. Sorokin, H. Lee, L. Y. Antipina, A. K. Singh, and B. I. Yakobson, "Calcium-decorated carbyne networks as hydrogen storage media," *Nano Letters*, vol. 11, no. 7, pp. 2660–2665, 2011. PMID: 21648444.

[12] N. W. Ashcroft and N. D. Mermin, *Solid State Physics*. Holt, Rinehart and Winston, 1968.

[13] L. A. Girifalco, M. Hodak, and R. S. Lee, "Carbon nanotubes, buckyballs, ropes, and a universal graphitic potential," *Phys. Rev. B*, vol. 62, pp. 13104–13110, Nov 2000.

[14] X. Zhao, Y. Ando, Y. Liu, M. Jinno, and T. Suzuki, "Carbon nanowire made of a long linear carbon chain inserted inside a multiwalled carbon nanotube," *Phys. Rev. Lett.*, vol. 90, p. 187401, May 2003.

[15] V. Babaev, M. Guseva, N. Novikov, V. Khvostov, and P. Flood, "Carbon material with a highly ordered linear-chain structure," in *Polyynes: Synthesis, Properties, and Applications* (F. Cataldo, ed.), CRC Press, 1st ed., 2005.

[16] Y. Kudryavtsev, S. Evsyukov, V. Babaev, M. Guseva, V. Khvostov, and L. Krechko, "Oriented carbyne layers," *Carbon*, vol. 30, no. 2, pp. 213–221, 1992.

[17] M. Guseva, V. Babaev, and N. Novikov, "Tetracarbon." WO 97/25078, July 17, 1997, December 18 1996.

[18] R. P. Feynman, "Space-time approach to non-relativistic quantum mechanics," *Rev. Mod. Phys.*, vol. 20, pp. 367–387, Apr 1948.

[19] A. Fetter and J. Walecka, *Quantum Theory of Many-particle Systems*. Dover Books on Physics, Dover Publications, 2003.

[20] N. Goldenfeld, *Lectures On Phase Transitions And The Renormalization Group*. CRC Press, 1st ed., 1992.

[21] L. D. Landau and E. M. Lifshitz, *Statistical Physics*. Pergamon Press, 3rd ed., 1980.

[22] M. Born and R. Oppenheimer, "Zur quantentheorie der molekeln," *Annalen der Physik*, vol. 389, no. 20, pp. 457–484, 1927.

[23] P. Hohenberg and W. Kohn, "Inhomogeneous electron gas," *Phys. Rev.*, vol. 136, pp. B864–B871, Nov 1964.

[24] M. Levy, "Universal variational functionals of electron densities, first-order density matrices, and natural spin-orbitals and solution of the v-representability problem," *Proceedings of the National Academy of Sciences*, vol. 76, no. 12, pp. 6062–6065, 1979.

[25] E. H. Lieb, "Density functionals for coulomb systems," *International Journal of Quantum Chemistry*, vol. 24, no. 3, pp. 243–277.

[26] W. Kohn and L. J. Sham, "Self-consistent equations including exchange and correlation effects," *Phys. Rev.*, vol. 140, pp. A1133–A1138, Nov 1965.

[27] J. P. Perdew and A. Zunger, "Self-interaction correction to density-functional approximations for many-electron systems," *Phys. Rev. B*, vol. 23, pp. 5048–5079, May 1981.

[28] J. P. Perdew, K. Burke, and M. Ernzerhof, "Generalized gradient approximation made simple," *Phys. Rev. Lett.*, vol. 77, pp. 3865–3868, Oct 1996.

[29] G. Kresse and J. Furthmüller, "Efficiency of ab-initio total energy calculations for metals and semiconductors using a plane-wave basis set," *Computational Materials Science*, vol. 6, no. 1, pp. 15–50, 1996.

[30] N. Troullier and J. L. Martins, "Efficient pseudopotentials for plane-wave calculations," *Phys. Rev. B*, vol. 43, pp. 1993–2006, Jan 1991.

[31] P. E. Blöchl, "Projector augmented-wave method," *Phys. Rev. B*, vol. 50, pp. 17953–17979, Dec 1994.

[32] "Pseudo potential by a. dal corso." http://pseudopotentials.quantum-espresso.org/upf_files/C.pbe-n-kjpaw_psl.1.0.0.UPF. Accessed on 11/9/2023.

[33] P. Giannozzi, S. Baroni, N. Bonini, M. Calandra, R. Car, C. Cavazzoni, D. Ceresoli, G. L. Chiarotti, M. Cococcioni, I. Dabo, A. D. Corso, S. de Gironcoli, S. Fabris, G. Fratesi, R. Gebauer, U. Gerstmann, C. Gougoussis, A. Kokalj, M. Lazzeri, L. Martin-Samos, N. Marzari, F. Mauri, R. Mazzarello, S. Paolini, A. Pasquarello, L. Paulatto, C. Sbraccia, S. Scandolo, G. Sclauzero, A. P. Seitsonen, A. Smogunov, P. Umari, and R. M. Wentzcovitch, "QUANTUM ESPRESSO: a modular and open-source software project for quantum simulations of materials," *Journal of Physics: Condensed Matter*, vol. 21, p. 395502, sep 2009.

[34] N. Marzari, D. Vanderbilt, A. De Vita, and M. C. Payne, "Thermal contraction and disordering of the al(110) surface," *Phys. Rev. Lett.*, vol. 82, pp. 3296–3299, Apr 1999.

[35] S. Cahangirov, M. Topsakal, and S. Ciraci, "Long-range interactions in carbon atomic chains," *Phys. Rev. B*, vol. 82, p. 195444, Nov 2010.

[36] M. Liu, V. I. Artyukhov, H. Lee, F. Xu, and B. I. Yakobson, "Carbyne from first principles: Chain of c atoms, a nanorod or a nanorope," *ACS Nano*, vol. 7, no. 11, pp. 10075–10082, 2013. PMID: 24093753.